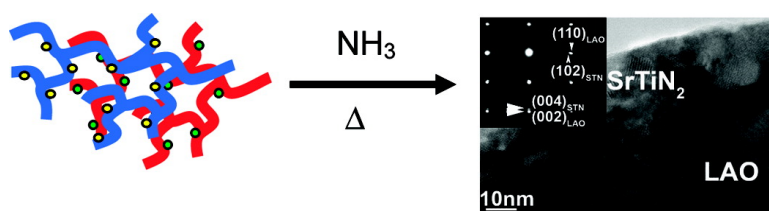


## Epitaxial Ternary Nitride Thin Films Prepared by a Chemical Solution Method

Hongmei Luo, Haiyan Wang, Zhenxing Bi, David M. Feldmann, Yongqiang Wang,  
 Anthony K. Burrell, T. Mark McCleskey, Eve Bauer, Marilyn E. Hawley, and Quanxi Jia

*J. Am. Chem. Soc.*, **2008**, 130 (46), 15224-15225 • DOI: 10.1021/ja803544c • Publication Date (Web): 22 October 2008

Downloaded from <http://pubs.acs.org> on February 8, 2009



### More About This Article

Additional resources and features associated with this article are available within the HTML version:

- Supporting Information
- Access to high resolution figures
- Links to articles and content related to this article
- Copyright permission to reproduce figures and/or text from this article

[View the Full Text HTML](#)

## Epitaxial Ternary Nitride Thin Films Prepared by a Chemical Solution Method

Hongmei Luo,<sup>\*,†</sup> Haiyan Wang,<sup>‡</sup> Zhenxing Bi,<sup>‡</sup> David M. Feldmann,<sup>†</sup> Yongqiang Wang,<sup>†</sup>  
Anthony K. Burrell,<sup>†</sup> T. Mark McCleskey,<sup>†</sup> Eve Bauer,<sup>†</sup> Marilyn E. Hawley,<sup>†</sup> and Quanxi Jia<sup>\*,†</sup>

Materials Physics and Applications Division, Los Alamos National Laboratory, Los Alamos, New Mexico 87545,  
and Department of Electrical and Computer Engineering, Texas A&M University, College Station, Texas 77843

Received May 13, 2008; E-mail: hluo@lanl.gov; qxjia@lanl.gov

Nitrides have been known to exhibit a number of important properties such as superconductivity, catalytic activity, unusual magnetic properties, and high hardness and mechanical strength.<sup>1–7</sup> Many studies have been focused on binary nitrides. Binary nitride and some mixed binary nitride films such as (Ti,Zr)N, (Ti,Nb)N, and (Zr,Nb)N have been prepared by physical or chemical vapor deposition.<sup>8,9</sup> Since the 1990s, ternary nitrides have attracted more attention. One of the commonly studied ternary nitride systems is AMN<sub>2</sub> (A = alkali metal, alkaline earth metal, or transition metal, and M = transition metal or lanthanide).<sup>10–15</sup> Two methods have been used to prepare these materials in bulk: a standard high temperature “ceramic method” by ammonolysis of oxides or binary nitrides, and the growth of submillimeter crystals from reactions containing molten metals as flux.<sup>3,4</sup> The development of a versatile technique for thin film deposition of ternary nitrides enables a wider range of technological applications. In this communication, we report the growth of epitaxial SrTiN<sub>2</sub> (STN) films using a chemical solution approach, polymer-assisted deposition (PAD).<sup>16–18</sup> Chemical solution deposition, where a precursor solution is deposited by spin- or dip-coating onto a single-crystal substrate,<sup>19</sup> has been successfully used to grow thin films of simple and complex oxides, as well as binary nitride GaN.<sup>20</sup> In the PAD process, the commercially available water soluble polymer not only controls the desired viscosity but also binds the metal ions to prevent premature precipitation and to form a homogeneous solution.<sup>18</sup>

To form epitaxial nitride films, we started with metal polymeric liquid precursors. The films were then thermally treated in ammonia gas to yield the metal nitride films. Briefly, the precursor for epitaxial STN films was a mixture of two separate Sr- and Ti-polymer solutions (see Supporting Information for details). The precursor solution was spin-coated onto (001) LaAlO<sub>3</sub> (LAO) substrates. The annealing was done in flowing ammonia gas at 1000 °C for 1 h.

As compared to LAO (pseudo cubic with a lattice constant  $a = 0.379$  nm), STN crystallizes in the tetragonal structure with a space group of  $P4/nmm$  ( $a = 0.388$  nm,  $c = 0.77$  nm).<sup>12</sup> Such a relatively small lattice mismatch makes it possible for STN films to grow epitaxially on LAO substrates. Figure 1 shows the X-ray diffraction (XRD) results from the  $\theta-2\theta$  scan and  $\phi$ -scans of an STN film on the LAO substrate. The presence of only the (004) peak from STN indicates that the film is preferentially oriented along the  $c$ -axis perpendicular to the substrate surface. It is noted that no detectable peaks from binary nitrides were observed in the XRD patterns. The in-plane orientation between the film and substrate was determined by XRD  $\phi$ -scans from the (204) of STN and (202) of LAO (see Figure 1b). The epitaxial relationships between the film and substrate can be deduced as  $(001)_{\text{film}} \parallel (001)_{\text{sub}}$  and  $[102]_{\text{film}} \parallel [101]_{\text{sub}}$

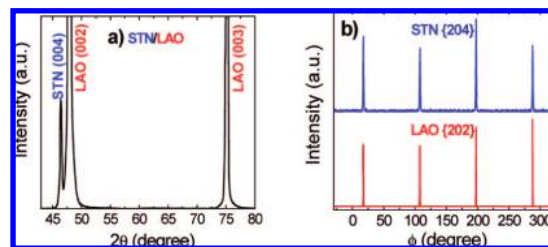


**Figure 1.** XRD patterns: (a)  $\theta-2\theta$  scan of a STN film on LAO; (b)  $\phi$ -scans from (204) reflection of STN and (202) reflection of LAO.

based on XRD  $\theta-2\theta$  and  $\phi$ -scans. An average full width at half-maximum (fwhm) value of  $1.1^\circ$  for STN, as compared to a value of  $0.7^\circ$  for the single crystal substrate, indicates the film to be of good epitaxial quality. The Rutherford backscattering spectrometry (RBS) analysis shows the Sr/Ti ratio in the STN film to be 0.8:1.0 as compared with the nominal predetermined ratio of 1.0:1.0 in the solution. It should be noted that a small amount of carbon and oxygen was detected in the films (Figure S1). Nevertheless, the carbon and oxygen contents are less than 10% based on such analysis.

It will be interesting to understand the growth mechanism of nitrides by treating the metal–polymer precursor in ammonia. The conversion of the metal–polymer precursor to nitrides is proposed to be controlled by the transamination process.<sup>21</sup> It is known that PEI can be completely depolymerized at high temperature when the precursors are treated in different environments.<sup>18</sup> Ammonia can be thermally decomposed to release various gaseous species ( $\text{NH}_2$ ,  $\text{NH}$ ,  $\text{N}_2$ ,  $\text{N}$ ,  $\text{H}_2$ , and  $\text{H}$ ) at temperatures higher than 600 °C.<sup>21,22</sup> In our PAD process, it is likely that the amine groups from ammonia decomposition replace the polymer to bind metals at high temperature through the transamination process.

The surface morphology and surface roughness of the films were investigated by both scanning electron microscopy (SEM) and atomic force microscopy (AFM). All the films are dense and smooth with no detectable microcracks (Figure S2). An AFM phase image of an STN film grown on LAO (Figure S3) indicates that the film has a root-mean-square (rms) surface roughness of  $\sim 6$  nm. Figure 2 shows the cross-sectional high resolution transmission electron microscopy (HRTEM) images of an STN film on an LAO substrate. The thickness of the STN film is  $\sim 35$  nm. It is clear that the interface between the nitride film and the substrate is clean. The corresponding selected area electron diffraction (SAED) pattern taken from the interface (see insert in Figure 2a) confirms the epitaxial growth of tetragonal STN film on LAO, evidenced by the distinct diffraction dots from the film and the substrate. The epitaxial relationships between the film and the substrate deduced from the SAED pattern are consistent with the XRD results.

First principle calculations predict that STN would show metallic.<sup>12</sup> Our ability to fabricate epitaxial STN films allowed us to

<sup>†</sup> Los Alamos National Laboratory.

<sup>‡</sup> Texas A&M University.

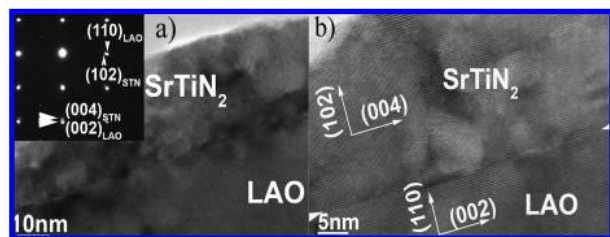


**Figure 2.** (a) A bright-field cross-sectional TEM image of an STN film on an LAO substrate. The inset shows the corresponding SAED pattern; (b) HRTEM image taken from the interface between the STN and the LAO.

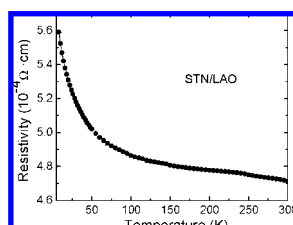


**Figure 3.** Temperature dependence of resistivity of an STN film on LAO.

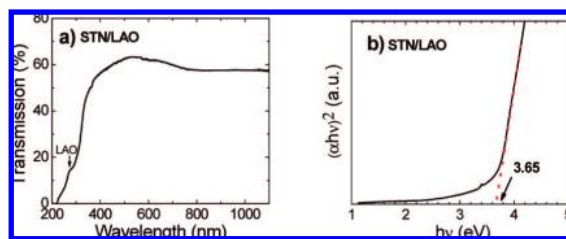


**Figure 4.** (a) Optical transmission spectrum of STN film on LAO; (b)  $(\alpha hv)^2$  versus  $hv$  plot for the determination of optical gaps of STN film on LAO, where  $\alpha$  is the absorption coefficient and  $hv$  is the photon energy.

investigate their physical properties. As shown in Figure 3, the STN film is conductive with a room temperature resistivity of  $\sim 4.7 \times 10^{-4} \Omega \cdot \text{cm}$  measured by a four-probe technique. Different from the first principle calculations, our epitaxial films show semiconductive resistivity vs temperature behavior, although the resistivity shows very weak temperature dependence in the range 300 to 50 K. Scattering from grain boundaries and carbon or oxygen contamination at the grain boundaries in the STN films can all contribute to such an effect, even though the XRD analysis has not revealed any detectable other phases. It should be noted that the STN powder prepared by the solid-state reaction did show the metallic behavior from 77 to 300 K; however, the STN powder contained 30 wt% Sr and SrO as impurities.<sup>12</sup>

Figure 4a shows the optical transmission characteristics of a 35 nm thick STN film on LAO. The film is transparent, having an optical transmission of  $\sim 60\%$  in the 400–1100 nm range. If we consider STN as a semiconductor based on the resistivity vs temperature behavior (see Figure 3), we can determine its optical band gap from the fundamental absorption, which corresponds to the electron excitation from the valence band to the conduction band. A sharp absorption edge was observed around 360 nm from STN, where the absorption around 270 nm was from LAO substrate

(Figure S4). Following Tauc's equation,<sup>23</sup> the optical band gap of a transparent semiconductor can be deduced from a plot of  $(\alpha hv)^m$  versus  $hv$ , where  $\alpha$  is the optical absorption coefficient,  $hv$  is the photon energy, and  $m$  depends on the type of transition:  $m = 2$  for a direct band transition and  $m = 1/2$  for an indirect band transition. A linear relationship between  $(\alpha hv)^2$  and  $hv$  (Figure 3b) indicates that the STN film has a direct energy band with a band gap of 3.65 eV by extrapolating the straight portion of the curve to  $(\alpha hv)^2 = 0$ . The band gap value indicates that our STN film behaves like a wide-band gap semiconductor.

In summary, we report the first growth of smooth epitaxial tetragonal ternary SrTiN<sub>2</sub> thin films by a chemical solution approach of polymer-assisted deposition. The PAD technique offers considerable promise for making complex nitride thin films by simply mixing the different metal polymer solutions. The epitaxial relationships between the film and the substrate are  $(001)_{\text{film}} \parallel (001)_{\text{sub}}$  and  $[102]_{\text{film}} \parallel [101]_{\text{sub}}$ . The films are conductive with a room temperature resistivity of  $4.7 \times 10^{-4} \Omega \cdot \text{cm}$ . At the wavelength in the range 400–1100 nm, the optical transmittance of the film is 60%. The energy band gap of semiconductive SrTiN<sub>2</sub> film is estimated to be 3.65 eV.

**Acknowledgment.** We gratefully acknowledge the support of the U.S. Department of Energy (DOE) through the LANL/LDRD Program, DOE EE-RE Solid State Lighting Program, and NSF/DMR Ceramic Program (NSF 0709831).

**Supporting Information Available:** Solution, film preparation, and characterization of nitride films. This material is available free of charge via the Internet at <http://pubs.acs.org>.

## References

- (1) DiSalvo, F. J. *Science* **1990**, *247*, 649.
- (2) Brese, N. E.; O'Keeffe, M. *Struct. Bonding (Berlin)* **1992**, *79*, 307.
- (3) DiSalvo, F. J.; Clarke, S. J. *Curr. Opin. Solid State Mater. Sci.* **1996**, *1*, 241.
- (4) Niewa, R.; Jacobs, H. *Chem. Rev.* **1996**, *96*, 2053.
- (5) Sriram, M. A.; Weil, K. S.; Kumta, P. N. *Appl. Organomet. Chem.* **1997**, *11*, 163.
- (6) Kniepp, R. *Pure Appl. Chem.* **1997**, *69*, 185.
- (7) Niewa, R.; DiSalvo, F. J. *Chem. Mater.* **1998**, *10*, 2733.
- (8) Boxman, R. L.; Zhitomirsky, V. N.; Grimberg, I.; Rapoport, L.; Goldsmith, S.; Weiss, B. Z. *Surf. Coat. Technol.* **2000**, *125*, 257.
- (9) Sandu, C. S.; Sanjines, R.; Benkahoul, M.; Medjani, F.; Levy, F. *Surf. Coat. Technol.* **2006**, *201*, 4083.
- (10) Gregory, D. H.; Barker, M. G.; Edwards, P. P.; Siddons, D. J. *Inorg. Chem.* **1998**, *37*, 3775.
- (11) Gregory, D. H.; O'Meara, P. M.; Gordon, A. G.; Siddons, D. J.; Blake, A. J.; Barker, M. G.; Hamor, T. A.; Edwards, P. P. *J. Alloys Compd.* **2001**, *317–318*, 237.
- (12) Farault, G.; Gautier, R.; Baker, C. F.; Bowman, A.; Gregory, D. H. *Chem. Mater.* **2003**, *15*, 3922.
- (13) Hunting, J. L.; Szymanski, M. M.; Johnson, P. E.; Kellar, C. B.; DiSalvo, F. J. *J. Solid State Chem.* **2007**, *180*, 31.
- (14) Gomathi, A. *Mater. Sci. Bulletin* **2007**, *42*, 870.
- (15) Mckay, D.; Hargreaves, J. S. J.; Rico, J. L.; Rivera, J. L.; Sun, X. L. *J. Solid State Chem.* **2008**, *181*, 325.
- (16) Jia, Q. X.; McCleskey, T. M.; Burrell, A. K.; Lin, Y.; Collis, G. E.; Wang, H.; Li, A. D. Q.; Foltyn, S. R. *Nat. Mater.* **2004**, *3*, 529.
- (17) Lin, Y.; Lee, J.-S.; Wang, H.; Li, Y.; Foltyn, S. R.; Jia, Q. X.; Collis, G. E.; Burrell, A. K.; McCleskey, T. M. *Appl. Phys. Lett.* **2004**, *85*, 5007.
- (18) Burrell, A. K.; McCleskey, T. M.; Jia, Q. X. *Chem. Commun.* **2008**, 1271.
- (19) Lange, F. F. *Science* **1996**, *273*, 903.
- (20) Sinha, G.; Ganguli, D.; Chaudhuri, S. J. *Colloid Interface Sci.* **2008**, *319*, 123.
- (21) Kisailus, D.; Choi, J. H.; Lange, F. F. *J. Cryst. Growth* **2003**, *249*, 106.
- (22) Yoshida, S.; Sasaki, M. J. *Cryst. Growth* **1994**, *135*, 633.
- (23) Tauc, J.; Grigorovici, R.; Yancu, Y. *Phys. Status Solidi* **1966**, *15*, 627.

JA803544C